Dynamic Spectrum Sharing Detectors

Karl N. Steadman, *Member, IEEE,* Ashley D. Rose, and Thao TN. Nguyen
Shared Spectrum Company
Vienna, VA 22182 USA
703-761-2818; fax: 703-761-2817
ksteadman@sharedspectrum.com

***Abstract*—Dynamic Frequency Sharing provides a mean to more efficiently allocate frequency spectrum. For this to be accomplished the ambient spectrum has to be sensed and characterized. This paper presents how energy detection can be used to differentiate signals from noise for various operating environments.**

Keywords-signal detection, noise measurement, DARPA XG, distributed frequency sharing, radio spectrum management, software defined radio

I. Introduction

XG technology enables a wireless networks to automatically select spectrum and operating modes that both minimize disruptions to existing users while optimizing operation of U.S. systems. This is accomplished in large part by sensing the ambient spectrum and detecting the presence of protected users. These users are operating radios which emit energy which can be detected. Reliable but sensitive detection of protected users enables sharing and pooling of dynamically available spectrum while not interfering with the existing spectrum stakeholders.

In this paper the performance of two implementations of detectors are studied relative to controlled signal and noise conditions. Further results show signal and noise environment for three environments. We characterized the choice of detection threshold for these measured environments for two thresholding schemes (absolute and relative).

Data for this report were collected through a series of three demonstrations. The next section describes the rational and execution of these demonstrations.

Manuscript received November 15, 2006. This work was supported in part by the U.S. Defense Advanced Research Projects Agency under Contract FA8750-05-C-0150.

II. False Alarm with White Noise Detection Test

A. Test Objectives

The objective of this test was to establish a baseline for the performance characteristics of the detection systems in a white noise environment. In the absence of any man-made noise, there is still thermal spectral energy that is referred to as background white noise. This is internally generated noise from the equipment itself. The internal thermal noise characteristic of the pre-selector, receiver and detector establishes the minimum usable noise floor setting for that detection system given a desired false alarm rate. Noise floor values are expressed in dBm/Hz and the smaller the value, the lower the noise and the more sensitive the detector.

In this test, the magnitude of the white noise was indirectly measured. The test correlates detection sensitivity with the Probability of False Alarms (P_{FA}). These measurements create a frame of reference from which subsequent testing and tuning can be judged. Once a target P_{FA} has been determined, the appropriate detector threshold can be established using this data.

B. Equipment, Software and Setup

Fig. 1 shows the equipment required and the test setup used to measure the various types of noise sensed by a detector. The detector was designed for the DARPA XG Program. Note that all equipment (cables, etc) was amplitude calibrated for all tests. This particular test, baseline false alarm rate with white noise, has the switch connected with the dummy load to avoid man-made noise and record only white, thermal noise.

The detector threshold for the XG Detector can be varied via a test script input, and the detector decision on whether a signal was / was not detected, along with the frequency bin, is recorded in a database. The test scripts were written to span the frequency range of 225 MHz to 575 MHz.

The two detectors tested were the Enhanced Rockwell Sensor [1] and the 1 MHz SSC detector. Both detectors use a windowed FFT to characterize the sampled signal to a 25 kHz resolution bandwidth. The Enhanced Rockwell Sensor has a 16 MHz instantaneous bandwidth while the SSC Detector has a 1 MHz instantaneous bandwidth. The 1 MHz design allowed the RF front-end to be designed with higher dynamic range, lower noise figure components. The SSC Detector was set to average over 2.56 ms, thus was proportionally slower than the Enhanced Rockwell Sensor.

Both detectors share a common antenna thus they are required to detect only during non-transmission periods of the host radio system. This requires careful time coordination with the network of host transmitters that is not discussed in this paper.

Metrics	Success Criteria
Detection probability vs Non-cooperative power spectral density	Pd=0.95 @ -178 dBm/Hz (-10 dB SNR with 6 dB NF) Pd=0.99 @ -163 dBm/Hz (5 dB SNR with 6 dB NF)
False alarm probability vs Non-cooperative power spectral density	Pfa=0.001 @ -178 dBm/Hz (-10 dB SNR with 6 dB NF) Pfa=0.0001 @ -163 dBm/Hz (5 dB SNR with 6 dB NF)
Prime power to scan 200 MHz, with 20 kHz BW, 10x/sec	1W

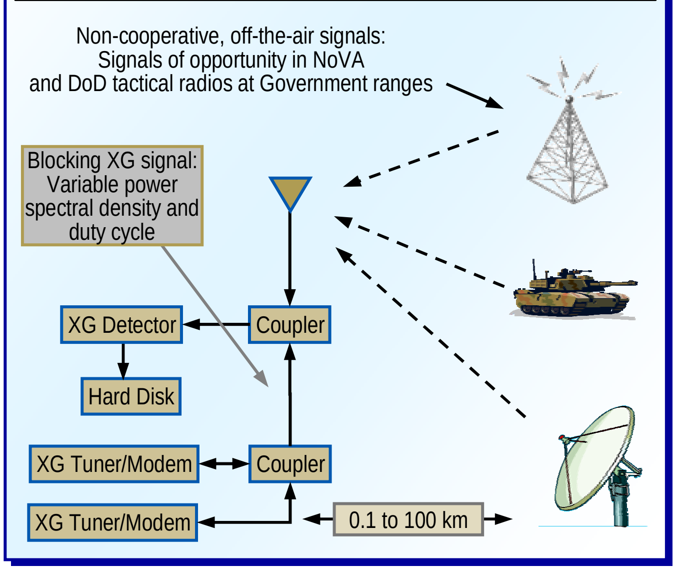

Figure 1. Detector Demonstrations: We identify the required detection and false alarm probability in multiple bands against many types of Non-Cooperative signals.

C. *Equipment Calibration*

Equipment calibration is critical because the detection results in absolute power levels are used in dynamic spectrum sharing algorithms. Each RF component was bar coded and assigned a unique test serial number for configuration management efficiency during field testing. The attenuation versus frequency was measured for each RF component at 10 MHz intervals, over the 30 MHz to 3 GHz frequency range. The resulting loss curve was saved for later analysis. The device's configuration number is associated with the loss curve.

D. *Output/Results*

It was expected that as the detector threshold is decreased, the P_{FA} will asymptote to 1. As the detector threshold is increased, the P_{FA} will asymptote to 0. The field collected data are compared with theoretical results of expected white noise and can be used in subsequent tests to set the minimum detection threshold. These tests show the best case sensitivities of the equipment are limited only by the internal thermal noise characteristics of the equipment itself.

Our experimental data was consistent with the predicted characteristics as shown in Fig. 2 for the Enhanced Rockwell sensor with the pre-selector. Fig. 3 shows the plot for the same measurement but for the SSC detector.

As expected the downward slope of the SSC Detector is much more abrupt as compared to the Enhanced Rockwell Sensor since it averages data. Also the lower noise figure of the SSC detector front end is represented by its respective lower knee in the false alarm curve. To obtain a false alarm rate of 10^{-4} the threshold of the Enhanced Rockwell Sensor would need to be -107 dBm while for the SSC Detector it would need to be -123 dBm.

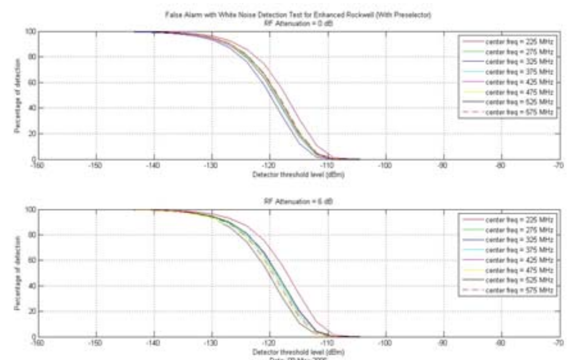

Figure 2. Enhanced Rockwell False Alarm White Noise Data Plot (with Pre-Selector).

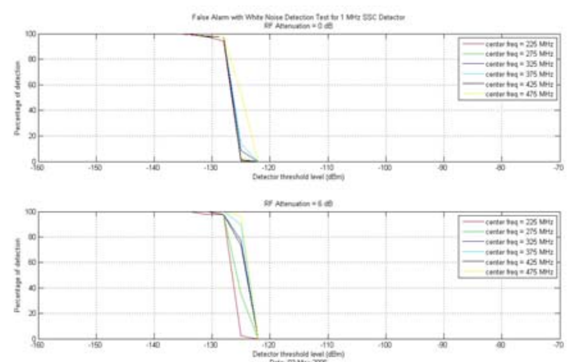

Figure 3. SSC Detector False Alarm White Noise Data Plot.

III. False Alarm with SPARK PLUG NOISE Detection Test

A. *Test Objectives*

This was very similar to the previous test, except that the objective was to determine the noise in the mobile test van (a Ford Econoline van) environment (in the SSC parking lot that is located in a dense urban area), and the corresponding required detector thresholds. While conducting mobile field tests using the test van, spark plug ignition noise has a potentially significant impact on the noise floor and required detector sensitivity thresholds. This test measured the noise floor of the detector in the presence of spark plug and other test van ambient noise. Spark plug noise and ambient white noise within the test van was measured by doing the experiment with an antenna. Noise from the mobile test van was recorded and was used for calibration purposes. Each detector has a different calibrated noise floor.

B. Equipment, Software and Setup

The equipment set-up was the same as the prior test.

Internal combustion engines idle at roughly 1000 RPM (Revolutions per Minute). Spark plug emissions on a six-cylinder engine should cause current spikes at a rate of 50 spikes per second. If the detector scans at a rate of 10 Hz, approximately 5 spikes per scan should appear. During drive tests, engines running between 2000 and 3000 RPM increase the spike rate to 100 to 150 spikes per second, or 10-15 spikes per scan.

C. Test Methodology

The detector was connected to the antenna on the van positioned in the SSC parking lot in Vienna, VA and measurements are made at idle and representative driving RPM. Detection measurements were made as described in the False Alarm with White Noise Detection test.

D. Output/ Results

Measurements were taken with both the Enhanced Rockwell sensor and the SSC Detector. There is an inherent difficulty with this particular experiment because it was not conducted in a signal free environment. Since the test was conducted in the parking lot at SSC, the antenna also picks up all ambient noise present in the local environment. While the effects of the spark plug noise were discernable, they were relatively small in scale. Fig. 4 shows the performance of the Enhanced Rockwell sensor in the presence of spark plug noise with the van operating at idle speed, while Fig. 5 is for driving RPM rates.

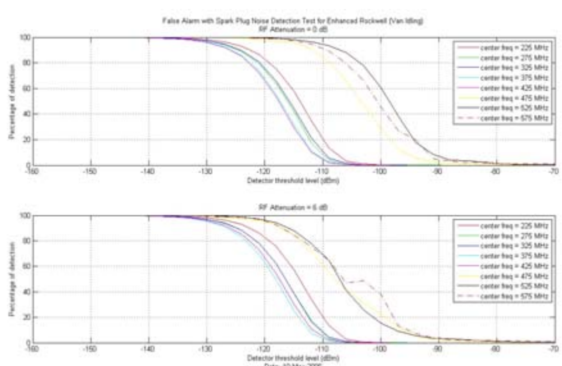

Figure 4. Enhanced Rockwell with Spark Plug Noise Pfa (Idle RPM).

The detection curves are reasonably consistent across the tested frequency range with some spikes that appear attributable to ambient environment phenomenon. The shape of the curves is consistent with the predicted behavior and the sensitivity is also on the order of what we expected in the -110 to -115 dBm range for the Enhance Rockwell sensor.

Using P_{FA} at -100 dBm is on the order of 10^{-5} for most of the frequencies tested. The three frequencies affected by the local ambient environment are on the order of 20 dB worse.

It appears that the spark plug noise in the tested frequencies is not a significant contributor to the overall noise level. Rather, the marked similarity to the other outside ambient noise data indicates the ambient environment is the dominating factor. The other reason is attributable to the limited set of frequencies sampled and the likelihood that more significant effects of spark plug noise would be seen in the 500 – 1500 kHz region of the spectrum.

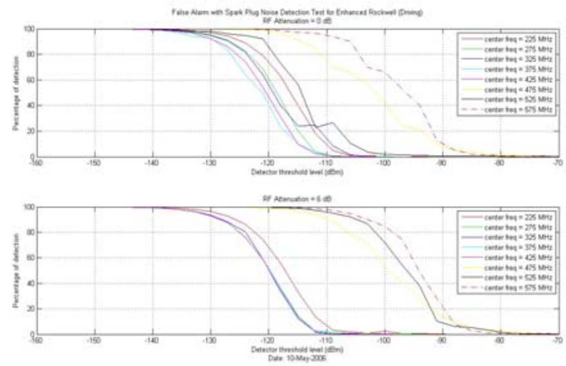

Figure 5. Enhanced Rockwell with Spark Plug Noise (Driving RPM).

The performance of the SSC Detector in the same condition is shown in Fig. 6. Again the SSC detector proved to be about 10 dB more sensitive than the Rockwell detector showing results in the -120 to -125 dBm range. The behavior was consistent with the predictions. On the log plot, P_{FA} of 10^{-5} is achieved as low as -123 dBm and at worst at -110 dBm; about 20 to 30 dB better than the Rockwell sensor.

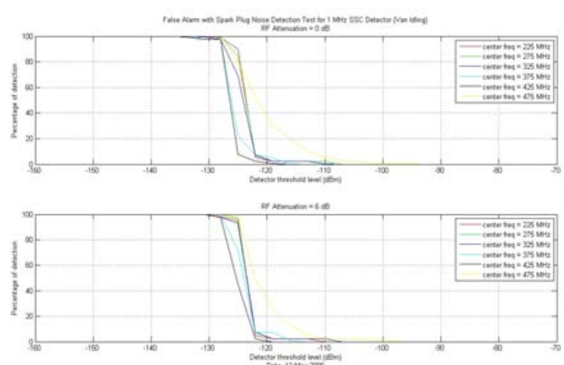

Figure 6. SSC Detector with Spark Plug Noise Pfa (Idle RPM).

IV. COMMERCIAL RADIO PROBABILITY OF DETECTION LAB TEST

A. Test Objectives

The objective of this test was to evaluate the capability of the detectors to sense various Non-Cooperative radio signal levels in a carefully calibrated lab environment. A sampling of Non-Cooperative radios was used to see the impact of different waveforms, and signal levels varied by applying attenuation. The XG detectors had varying levels of sensitivity thresholds to verify the detection of weak Non-Cooperative signals. The Probability of Detection (P_D) was determined.

B. Equipment, Software and Setup

Fig. 1 shows the equipment and the test setup used to measure the ability of the detectors to sense Non-Cooperative signals. The equipment (cables, attenuation matrix, etc) was calibrated as discussed previously. This test was performed in the laboratory to carefully control the signal levels.

The detector threshold was varied via a test script input, and the detector decision whether a signal was / was not detected, along with the frequency bin, was recorded in a database. The test script also controlled the attenuation matrix, which was used to simulate a weak signal situation. Finally, the test scripts, via a relay board, also controlled when the Non-Cooperative radio transmits.

C. Output/ Results

The Enhanced Rockwell Sensor probability of detection plot for a land mobile FM ICOM Land Mobile radio is shown in Fig. 7. Each chart shows the probability of detection vs. the required signal strength for different detection threshold levels. The data are consistent across the three radio types, and with the predicted behavior discussed in the previous paragraph.

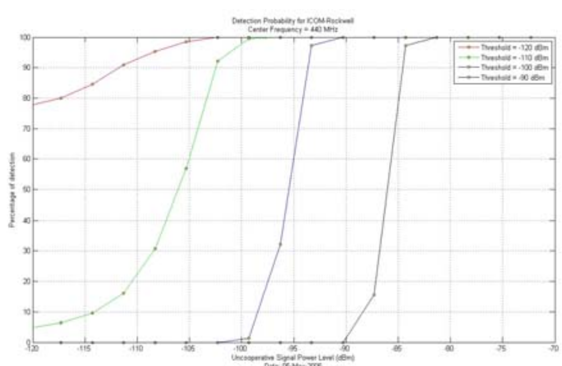

Figure 7. Enhanced Rockwell Sensor P_D for the ICOM Signal.

The same series of tests were conducted with the SSC detector. Fig. 8 shows the SSC detector performance against the CW signal for each of the four detector thresholds. The curves are markedly steeper and more uniform than the Rockwell sensor against the same signal source. The performance of the SSC detector is at least 5 dB better. Fig. 8 shows the SSC detector performance against the ICOM Land Mobile Radio.

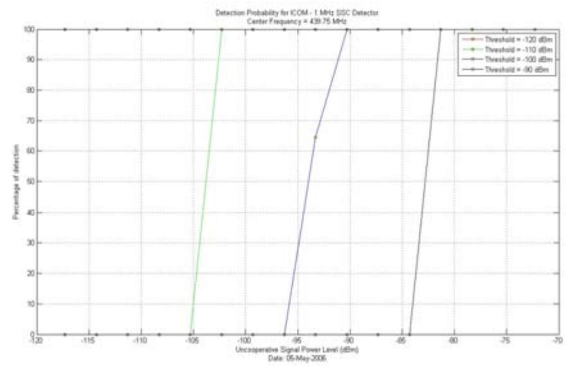

Figure 8. SSC Detector P_D for the ICOM Signal.

V. SIGNAL AND NOISE CHARACTERIZATION FIELD TESTS (225-500MHz)

A. Test Objectives

The objective of this test was to collect field spectrum data to characterize separating noise from signal events for three cases of environments. One environment is rural where there is a minimum of RF transmitters. In particular we traveled to Green Bank, WV to the National Radio Astronomy Observatory which is designated as an 'RF quiet zone'. Other environments are expected to have progressively more ambient signals and noise with semi-rural (Fort A.P. Hill, VA) and suburban (Ashburn, VA).

B. Equipment, Software and Setup

The equipment required and the test setup is described next. Ambient signals are received by an omni-directional discone antenna which operates from 25 MHz to 1300 MHz. These signals were connected to the Sentinel subsystem through 3.7 meters of low loss RF cable.

The Sentinel subsystem as shown in Fig. 9 encompasses a laptop computer running software which gathers data to be stored on an external hard drive which is collected by an Enhanced Rockwell Sensor. These devices are connected by an Ethernet cable. In the same box is a GPS receiver (Thales) used to determine the latitude, longitude, and elevation of the subsystem. All these components are mounted in a metal enclosure with a removable lid with an RF gasket. A fan provides forced air cooling through a fine meshed RF screen. It was verified that the metal enclosure shields the emissions from the laptop for being received by the antenna.

Signals are collected inside the Sentinel subsystem using an Enhanced Rockwell Sensor. This sensor is set to operate from 225 to 500 MHz. A resolution bandwidth of 25 kHz was used with no video averaging. The Rockwell Sensor has an instantaneous bandwidth of 16 MHz. The sensor collects time samples within this subband, uses a Blackman window, and performs a FFT, prior to moving on to the next adjacent subband until it scans the complete continuous 225 to 500 MHz band.

The raw Enhanced Rockwell Sensor spectra trace is shown on the top pane of Fig. 10. This data was recorded over approximately 10 minutes while it was connected to a dummy load. We see two signal artifacts. The plot shows spectra lines caused by internal spurs. These spurs are products of the local oscillator being mixed into the sampled passband. Secondly, the transfer function of the instantaneous bandwidth can be seen periodically across the sampled spectrum, as shown in the second pane after we removed the spectra peaks. Through signal processing we estimate this transfer function and through its inverse compensate for its effect. After this processing we obtain the bottom pane of Fig. 10.

The data is processed by a laptop located within the same Sentinel enclosure. The laptop processor requests a complete swept scan of frequency about ten times a second. This data is stored on its hard drive in a compact binary format for later analysis.

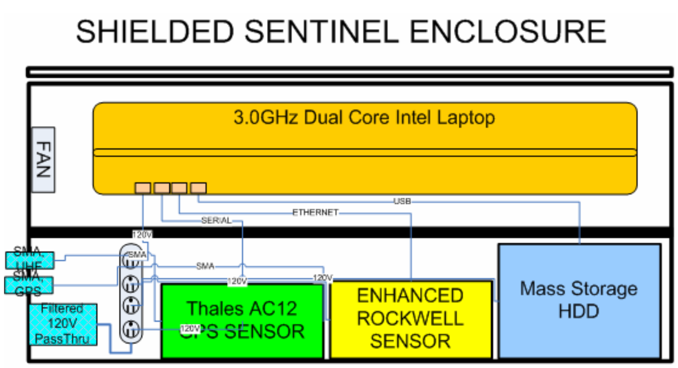

Figure 9. Sentinel Subsystem.

C. Test Methodology

Off-the-air signal testing was made over the frequency range 225 to 500 MHz and tested a wide range of signals in non-Gaussian noise environments. The steps followed were:

The test setup as described in the previous section is loaded onto a van. The van was driven to a designated scenario environment and parked for three hours. During these three hours the Sentinel scanned the ambient spectrum. The Sentinel was running off battery power to minimize prime generation RFI. The time of the test was logged as well the position of the van using a GPS receiver.

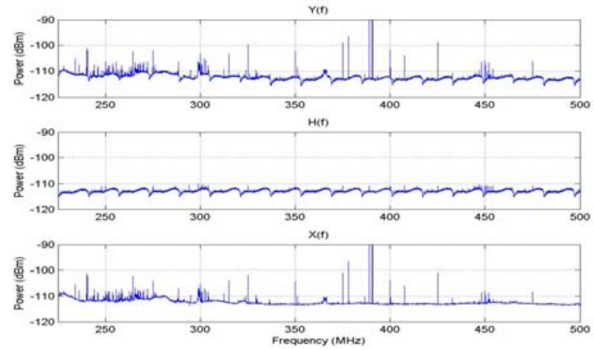

Figure 10. Enhanced Rockwell Sensor Exhibiting Both Subband Transfer Function and Spurious Signals.

D. Output/ Results

Data at each location is represented as a pair of figures. The first figure shows all the signal events and the average power for three hours in 225 to 500 MHz range. The second figure shows percentage of available bandwidth for a 1.75 MHz signal for different values of threshold. In the top pane, three thresholds were used -110 dBm, -105 dBm, and -100 dBm. In the bottom pane, the three values of threshold were set marginal to the minimum noise floor level at a 25 kHz bin for a 21 MHz subband. Three margin values are 5 dB, 10 dB, and 15 dB. This data is shown in Fig. 11 to Fig. 16.

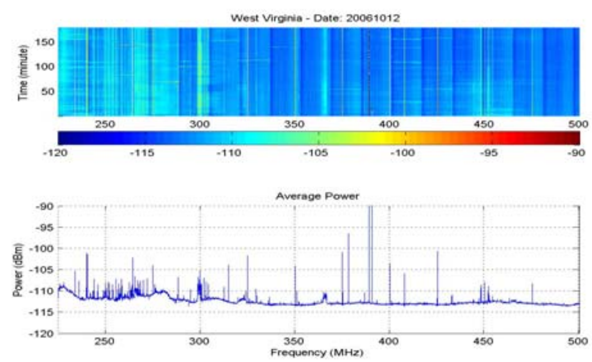

Figure 11. West Virginia 225 MHz - 500 MHz Spectrum Characteristics.

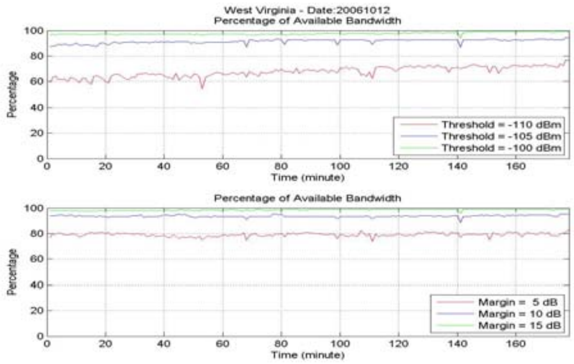

Figure 12. West Virginia 225 MHz - 500 MHz Percentage of Available.

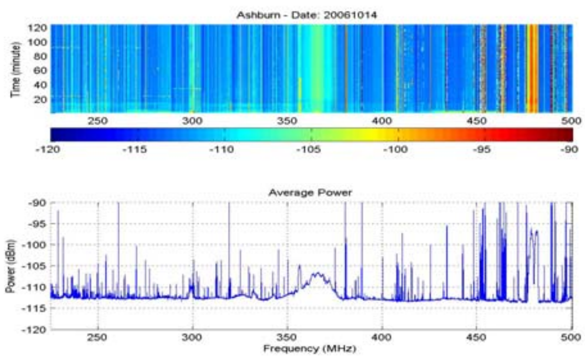

Bandwidth.

Figure 13. Ashburn, VA 225 MHz - 500 MHz Spectrum Characteristics.

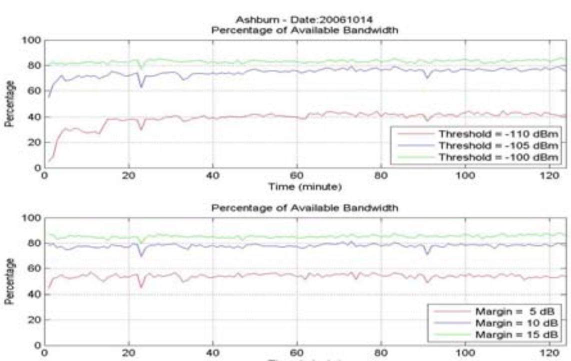

Figure 14. Ashburn, VA 225 MHz - 500 MHz Percentage of Available Bandwidth.

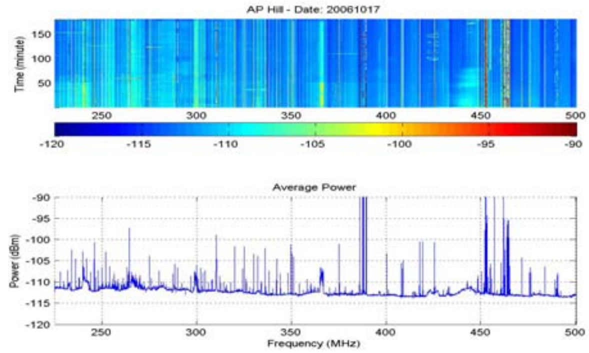

Figure 15. Fort A.P. Hill 225 MHz - 500 MHz Spectrum Characteristics.

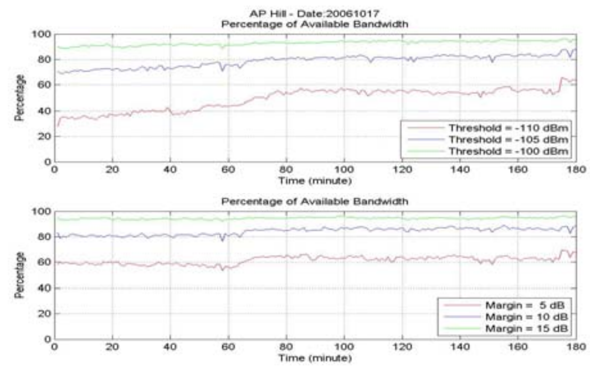

Figure 16. Fort A.P. Hill 225 MHz - 500 MHz Percentage of Available Bandwidth.

We note that as expected there are more signal present at larger power levels at the urban location (Ashburn) compared to the rural location (West Virginia). A threshold of -105 dBm provides a frequency reuse of 60% of spectrum in all the environments. There is a small variance in the amount of frequency in reuse over the three hour period.

A fixed threshold harvests similar percentages of white space (1.75 MHz signal bandwidth) as the method based on a margin above a threshold except for the lowest margin case. The lowest margin allows for a slight improvement in sensing available spectrum and at an improved sensitivity value.

VI. CONCLUSION

A dynamic spectrum sharing radio system uses a wideband detector to sense the ambient RF environment in order to dynamically adjust its transmit channel. This capability is limited by the minimum detector threshold that can be used with a reasonable false alarm level.

In this paper we compared the probability of false alarm and probability of detection for two detectors with significantly different operating characteristics. We analyzed two methods to get the threshold level for energy detector using data obtained from representative environments.

We showed that the ambient noise is a major limitation to a detector in an urban environment in the 225-500 MHz frequency range. A successful detector will have to use sophisticated detection algorithms to operate with reasonable sensitivity in this band. This will be a major challenge for DoD, public safety and TV band sharing which are close in frequency to our test frequency range.

We measured the P_D and P_{FA} curves for a typical land mobile radio. These curves are critical in predicting the performance of a dynamic spectrum sharing radio that operates in spectrum currently used by this type of narrow bandwidth (25 kHz), voice radio.

We made estimates of the amount of spectrum available to a dynamic spectrum sharing radio using a wide bandwidth (1.75 MHz) signal versus time in a three hour period and with different detection threshold levels. There is a significant amount of spectrum available using a low threshold (-110 dBm). The amount varies with time and with location.

We continue to process these same data using an Amplitude Probability Distribution method [5] to find methods to obtain lower thresholds in complex, urban RF environments.

REFERENCES

[1] "Interface control document for the XG enhanced sensor module phase II", Rockwell Collins Inc., Cedar Rapids, Iowa, 2005, unpublished.

[2] S. M. Kay, "Fundamentals of statistical signal processing: Detection theory", vol. 2, Prentice Hall, 1998.

[3] "Technical report – Study/Services, Demonstration result report", Shared Spectrum Company, Vienna, VA, 2006.

[4] M. McHenry, "Dynamic spectrum sharing," presentation to the Northern Virginia chapter of IEEE Comsoc, Jan. 25, 2005. Available: http://www.sharedspectrum.com/?section=presentations

[5] D. Middleton, "Statistical-physical models of man-made and natural radio-noise environment - Part III: First-order probability models of the instantaneous amplitude of Class B interference", NTIA Contractor report 78-1, June1978.